



LAWRENCE  
LIVERMORE  
NATIONAL  
LABORATORY

# Effect of NLTE emissivity models on NIF ignition hohlraum power requirements

L. Suter, S. Hansen, M. Rosen, P. Springer, S.  
Haan

June 16, 2009

Atomic Processes in Plasmas Conference  
Monterey, CA, United States  
March 22, 2009 through March 26, 2009

## **Disclaimer**

---

This document was prepared as an account of work sponsored by an agency of the United States government. Neither the United States government nor Lawrence Livermore National Security, LLC, nor any of their employees makes any warranty, expressed or implied, or assumes any legal liability or responsibility for the accuracy, completeness, or usefulness of any information, apparatus, product, or process disclosed, or represents that its use would not infringe privately owned rights. Reference herein to any specific commercial product, process, or service by trade name, trademark, manufacturer, or otherwise does not necessarily constitute or imply its endorsement, recommendation, or favoring by the United States government or Lawrence Livermore National Security, LLC. The views and opinions of authors expressed herein do not necessarily state or reflect those of the United States government or Lawrence Livermore National Security, LLC, and shall not be used for advertising or product endorsement purposes.

## Effect of NLTE emissivity models on NIF ignition hohlraum power requirements

L. Suter, S. Hansen\*\*, M. Rosen, P. Springer, S. Haan

Lawrence Livermore National Laboratory, Livermore, CA, \*\*present address, Sandia National Laboratory, Albuquerque, NM

*NLTE atomic physics models can significantly affect the power requirements and plasma conditions in ignition hohlraums. This is because the emissivity is a significant factor in determining the time dependent coronal temperature of the hot blow-off plasma filling ignition hohlraums, which, in turn, determines the total energy stored in that coronal plasma at any instant. Here we present best estimates of NLTE emissivity using the SCRAM model, including the range of uncertainty, and compare them with the emissivity of the model used to design NIF ignition hohlraums and set the NIF pulse shape, XSN NLTE. We then present pulse shapes derived from hohlraum simulations using an atomic physics model that approximates the SCRAM emissivities. We discuss the differences in coronal energetics and show how this affects the pulse shape and, in particular, the peak power requirement.*

For some time we have been examining the effect of atomic physics models on estimated laser requirements for NIF (National Ignition Facility) ignition targets. Here we discuss the effect of two different non-LTE atomic physics models on the power and energy requirements. One model is XSN-NLTE [1], a time dependent average atom model which has a good record for successfully modeling the radiation environment in Nova, Omega and NEL (NIF Early Light) hohlraums [2, 3, 4, 5, 6]. XSN-NLTE is a “production” atomic physics model that has sufficient computational efficiency that it can be run in-line in radiation-hydrodynamics target design codes, such as LASNEX [7]. XSN-NLTE has been used to design virtually all targets for NIF. The second model is SCRAM NLTE [8], a hybrid atomic-structure model that uses fine structure for singly excited coronal state while highly excited states and extensive configurations are included but not treated in detail. SCRAM includes selective averaging that minimizes impact on accuracy. SCRAM is a more rigorous atomic physics model than XSN-NLTE but is vastly less efficient computationally. It cannot realistically be run in-line in a radiation hydrodynamics design code.

In the work reported here, the key difference between SCRAM and XSN-NLTE is their emissivities (the rate at which an optically thin plasma produces radiation/cc). Figure 1 plots NLTE emissivity vs electron temperature ( $T_e$ ), for Au at a density of  $10\text{mg/cm}^3$  (corresponding to  $n_e/n_c \sim 0.2$ , an important coronal density in ignition hohlraums). The emissivities plotted here do not include photoexcitation of radiating levels due to a background radiation field. They only show the emissivity due to collisional processes. Plotted are the XSN-NLTE emissivity (line at bottom of figure) and three values of SCRAM emissivity (dashed lines). The three SCRAM curves correspond to the best estimate of Au emissivity in this range of temperature and density and estimated upper and lower bounds on emissivity based on model uncertainty assessments informed by results from other state-of-the-art models from a recent NLTE kinetics workshop [9]. The figure shows the more rigorous SCRAM emissivity to be significantly higher than

XSN-NLTE's, especially at lower electron temperatures due to the greatly increased number and types of transitions that are allowed. The emissivity here decreases with increasing temperature as the closed-shell Ni-like ion becomes the dominant species.

In order to assess the effect of different emissivity models on laser requirements, we performed a series of 1D simulations of an ignition capsule implosion inside a laser heated hohlraum; see figure 2. Our design for this study is a NIF "ignition candidate" target known as Rev3, a Ge-doped CH capsule driven by the shaped radiation temperature  $T_R(t)$  also shown in figure 2 [10]. The capsule outer radius is 1125  $\mu\text{m}$ . We place the capsule inside a spherical hohlraum with an initial inner radius of 4106  $\mu\text{m}$ , giving a case:capsule ratio of 3.65; a value typical of NIF ignition targets. To mock-up radiation losses through laser entrance holes, we extract radiation from the volume of the 1D hohlraum at a rate of  $\sigma T_R^4 A_{LEH}$ , where  $\sigma$  is the Stephan-Boltzman constant and  $A_{LEH}$  is the correct area of the laser entrance holes (equal to  $\sim 6\%$  of the hohlraum's wall area). The wall of the hohlraum consists of relatively thick U with a 0.4  $\mu\text{m}$  anti-oxidation layer of Au on the inside of the U. Because the laser never fully burns through this 0.4  $\mu\text{m}$  Au layer, all the NLTE physics will occur in Au plasma created from this thin layer. Consequently, our calculations vary the NLTE atomic physics model only in the thin Au layer. The thick U wall, which is diffusively heated by the hohlraum's radiation field remains LTE, allowing us to simulate the thick wall with a fixed LTE model (STA) in all our studies.

For each NLTE model we adjusted the laser power vs time incident upon the hohlraum wall in the 1D simulation (cf figure 2) until the hohlraum's radiation temperature vs time closely approximated the desired temperature versus time. Indeed, the  $T_R$  versus time plot of figure 2 is an overlay of four  $T_R(t)$ 's resulting from tuning laser power with the four NLTE emissivities studied. As previously mentioned, SCRAM atomic physics cannot be directly incorporated as an in-line atomic physics model in a code like LASNEX. Therefore, in our LASNEX simulations, SCRAM's NLTE emissivities vs  $T_e$  were approximated by using a "tuned" version of XSN. This tuning was accomplished by turning on two-electron recombination physics in XSN and then adjusting the rate multipliers [11]. The resulting emissivities used to approximate SCRAM in this study are the thin lines in figure 1 that roughly approximate the dashed SCRAM curves.

Figure 3 shows the bottom line of this study, that the laser power versus time requirements can be significantly affected by the NLTE emissivity. The peak power required by XSN-NLTE is some 60-80TW higher than the peak power that would be required when calculated with SCRAM-like emissivities. Complementing these 1D hohlraum simulations were a set of simulations to independently verify that changing the atomic physics model of the thin-Au layer did not significantly affect the x-ray energy that diffused into the hohlraum wall. We found the total energy of x-rays "lost" to the hohlraum wall to be 595kJ when modeling the thin-Au layer with XSN-NLTE and 599kJ when modeling with SCRAM-like NLTE. This is not surprising since the bulk of the radiation lost to the wall ends up in the thick U layer which is LTE STA in all cases. Because the x-ray energy absorbed by the capsule and escaping the LEH's is also about the same for all cases (identical  $T_R(t)$ 's) the total x-ray energy produced in each

simulation must be about the same (since the wall, capsule and LEH are the only sinks of x-ray energy). However, figure 3 shows the total laser powers and energies to be different. Since the thermal x-ray power and energy into the capsule, wall and LEH are the same but the required laser power and energy is different, the difference must be power and energy going into the hot corona inside the hohlraum.

We can analyze our LASNEX simulations to separate the energy in the problem into thermal energy and coronal energy. (See Appendix A for a discussion of the methodology.) The coronal energy represents energy absorbed from the laser that has not been converted into x-rays. Figure 4 plots the coronal energy vs time in our simulated hohlraum for the four NLTE atomic-physics models studied. We see that for XSN-NLTE the coronal energy peaks at about 340kJ (out of ~1000 kJ of total laser energy) and then drops to about 230 kJ after the laser turns off. The drop represents coronal energy that is being converted to x-rays. With SCRAM-like NLTE models, the coronal energy is lower. The NLTE model that corresponds to SCRAM's most-likely emissivity has a peak coronal energy some 80kJ less than XSN-NLTE and final coronal energy about 30kJ less. The NTE model corresponding to SCRAM's upper-bound on emissivity has a peak coronal energy some 150kJ < XSN-NLTE and a final energy that is ~90kJ less.

In figure 4 the slope of the coronal energy vs time curves represents the laser power vs time needed to create and heat the coronal plasma filling the hohlraum. At 17.5 ns, the XSN-NLTE coronal plasma "soaks up" ~150 TW, while the SCRAM-like nominal and upper bound NLTE coronas require ~80 and 60 TW, respectively. The difference in power going to the corona is the cause of the difference in total power requirements shown in figure 3.

Further analysis of the simulations shows that the difference in corona energies for the different models is reflected in different average corona temperatures and masses of corona plasma. The peak mass-average electron temperature for XSN-NLTE is 3.4keV at peak power and 1.4keV at the end. With the nominal SCRAM-like NLTE model the mass average coronal temperature is 2.9keV peak and 1.4keV at the end. The mass of material in the corona is ~1.8 mg for XSN-NLTE and ~1.5mg for the nominal SCRAM-like NLTE. These differences in temperatures and masses are a direct result of the differences in emissivities of figure 1. Greater emissivity can result in a coronal blow-off that is cooler and has less mass.

As mentioned earlier, XSN-NLTE has a very good record for modeling drive in Nova and Omega hohlraums. We note that Nova/Omega hohlraums are less than to approximately 1/3 the physical size of NIF ignition hohlraums, such as the one modeled here. Since the hohlraum volume:surface area ratio scales with the size of the hohlraum, the fraction of total energy stored in the corona versus the fraction in the walls and capsule is significantly greater on NIF than on Nova; 20-30% on NIF versus 5-10% on Nova. Because of this, NIF hohlraums are more sensitive to models which change the coronal energy than previous Nova/Omega hohlraums. We intend to look for this effect on our earliest NIF experiments.

This work was prepared by LLNL under Contract DE-AC52-07NA27344.

## Appendix A: Partitioning energy in a simulation into thermal and coronal energy

This partitioning is simplified by the observation that in simulated hohlraums only a very small fraction of the total energy in the simulation is in matter with electron temperature between  $T_r$  and several hundred eV hotter than  $T_r$ . Consequently, we can define a corona threshold temperature,  $T_{\text{corona\_threshold}}$ , some 100eV hotter than the peak  $T_r$ . We then define corona energy as that energy in plasma with  $T_e > T_{\text{corona\_threshold}}$ . Since there is virtually no energy with  $T_e$  between  $T_r$  and  $T_{\text{corona\_threshold}}$  we equate the energy in matter having  $T_e < T_{\text{corona\_threshold}}$  with the thermal energy in the wall and ablator. In the calculations this energy proves to be indistinguishable from what would, in very simple hohlraum models, be considered energy in material heated by x-radiation. The corona energy represents energy that has been directly absorbed from the laser and has not been converted into x-rays. In simple models of hohlraums it can be thought of as  $(1-\eta_{\text{CE}})E_{\text{laser}}$  where  $\eta_{\text{CE}}$  is the x-ray conversion efficiency; the fraction of laser energy converted into x-rays. For completeness we note that our methodology for tracking the time dependent evolution of corona energy includes a small correction when a mass element is “promoted” into the corona as it heats up. The energy it had up until the instant of promotion came from x-radiation and represents laser energy that did get converted to x-radiation. The corona energy associated with that mass-element is only the energy that is acquired after the promotion.

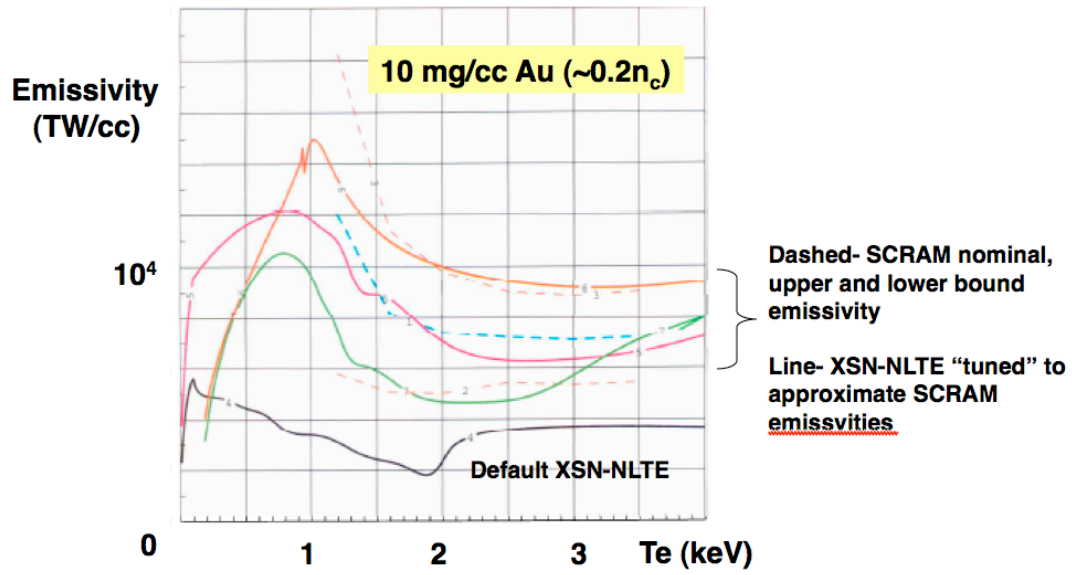


Figure 1- NLTE emissivity vs electron temperature in the four models studied. Curves shown were generated in an optically thin plasma with no radiation field. Emission is due solely to collisional processes.



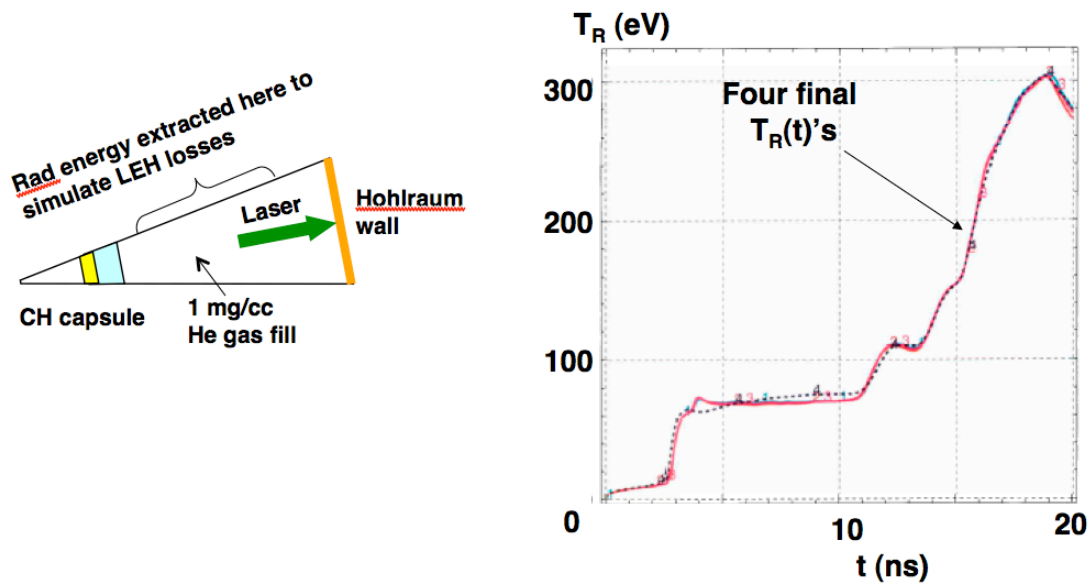


Figure 2- Left: Our 1D integrated hohlraum simulations included a 1-D laser source; a CH capsule; 1mg/cc He gas fill; LEH losses; a hohlraum wall composed of  $19.6\text{ }\mu\text{m}$  U (LTE STA) with an inner  $0.4\text{ }\mu\text{m}$  Au anti-oxidation layer. The NLTE models studied were used only in the  $0.4\text{ }\mu\text{m}$  Au layer. The laser never fully burns through the thin Au layer. Right: For each NLTE model the laser power vs time was tuned to provide the “Rev3-like”  $T_R(t)$  shown.

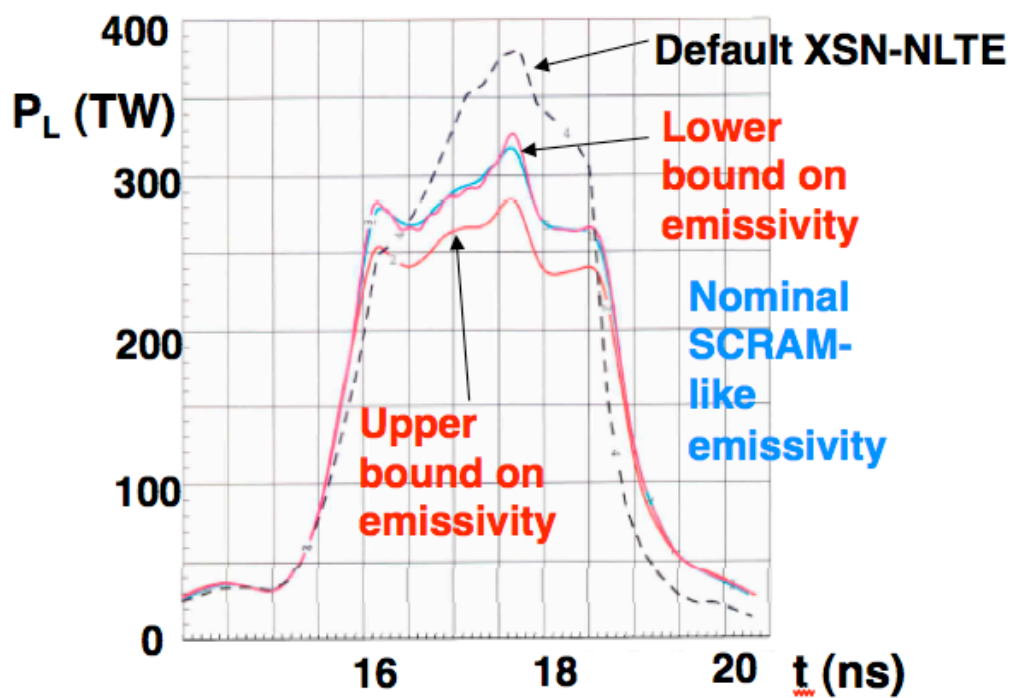


Figure 3- Laser power required to produce the Rev3-like  $T_R(t)$  with each of the four NLTE emissivity models studied

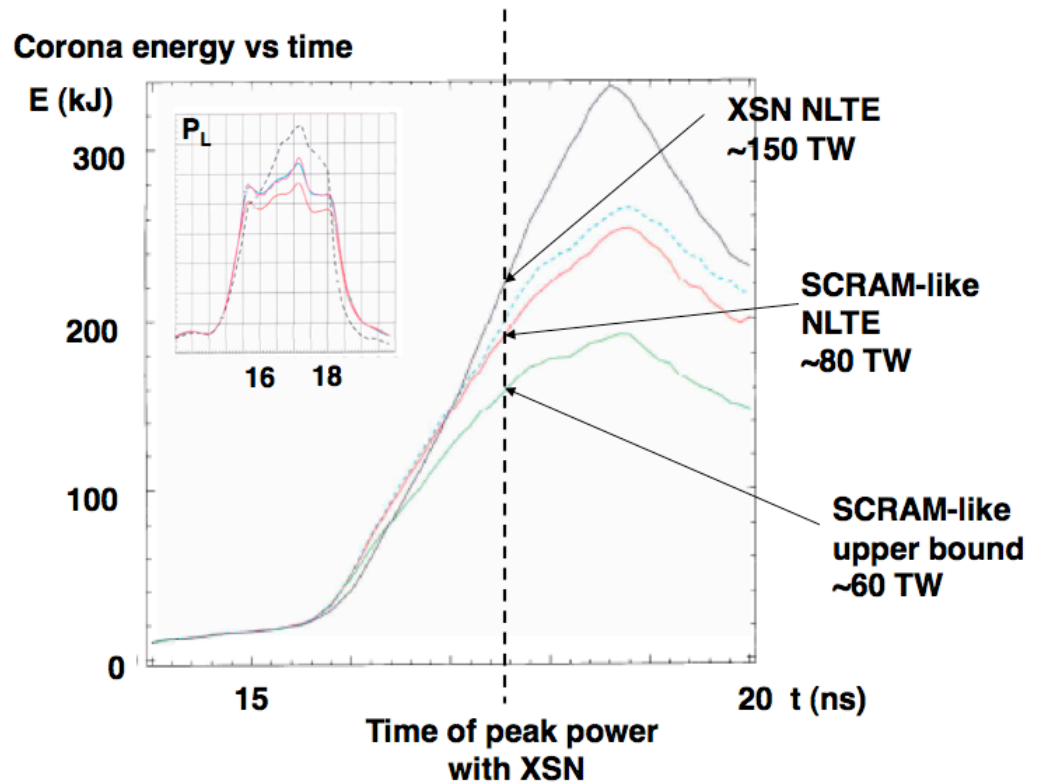


Figure 4- Corona energy vs time for the four NLTE emissivity models studied. Total laser energy is ~1000 kJ. In NIF ignition targets the energy stored in the corona is a substantial fraction of the total laser energy.

## References:

- 1- D. E. Post, R. V. Jensen, C. B. Tarter, W. H. Grasberger, and W. A. Lokke, *At. Data Nucl. Data Tables* 20, 397 (1977).
- 2- E. Dattolo, L. Suter, M. C. Monteil, J. P. Jadaud, N. Dague, et. al. , *Phys. Plasmas* 8, 260 (2001).
- 3- E. L. Dewald, L. J. Suter, O. L. Landen, et. al., *Phys. Rev. Lett.* 95, 215004 (2005)
- 4- See National Technical Information Service Document No. DE00008491 [L. J. Suter, E. Dattolo, S. Glenzer, J.-P. Jadaud, R. Turner, N. Dague, C. Decker, M.-C. Monteil, O. Landen, D. Juraszek, B. Lasinski, and B. J. MacGowan, “Understanding and Modeling of Ignition Hohlraum X-ray Coupling Efficiency,” Lawrence Livermore National Laboratory UCRLRL- 105821-98-4 (1998), p. 171]. Copies may be obtained from the National Technical Information Service, Springfield, VA 22161.
- 5- L. J. Suter, R. L. Kauffman, C. B. Darrow et al., *Phys. Plasmas* 3, 2057 (1996).
- 6- R. L. Kauffman, L. J. Suter, C. B. Darrow et al., *Phys. Rev. Lett.* 73, 2320 (1994).
- 7- G. B. Zimmerman and W. L. Kruer, *Comments Plasma Phys. Control. Fusion* 2, 51 (1975).
- 8- S.B. Hansen, J. Bauche, C. Bauche-Arnoult, and M.F. Gu, *HEDP* 3, 109 (2007)
- 9- C.J. Fontes, J. Abdallah Jr., C. Bowen, R.W. Lee, and Yu. Ralchenko, *HEDP* 5, 15 (2009)
- 10- S. Haan, private communication (LLNL, 2007).
- 11- G. Zimmerman, J. Castor, private communication (LLNL, 2008).